forests

MDPI

Article

Transcriptome Analysis in Male Strobilus Induction by Gibberellin Treatment in *Cryptomeria japonica* D. Don

Manabu Kurita [1,†], Kentaro Mishima [2,*,†], Miyoko Tsubomura [2], Yuya Takashima [2], Mine Nose [2], Tomonori Hirao [2] and Makoto Takahashi [2]

1 Kyushu Regional Breeding Office, Forest Tree Breeding Center, Forestry and Forest Products Research Institute, Forest Research and Management Organization, 2320-5 Suya, Koshi, Kumamoto 861-1102, Japan; mkuri@affrc.go.jp

2 Forest Tree Breeding Center, Forestry and Forest Products Research Institute, Forest Research and Management Organization, 3809-1 Ishi, Juo, Hitachi, Ibaraki 319-1301, Japan; mtsubo@affrc.go.jp (M.T.); ytakashima@ffpri.affrc.go.jp (Y.T.); minenose@affrc.go.jp (M.N.); hiratomo@affrc.go.jp (T.H.); makotot@affrc.go.jp (M.T.)

* Correspondence: mishimak@affrc.go.jp

† Contributed equally.

Received: 13 May 2020; Accepted: 1 June 2020; Published: 3 June 2020

Abstract: The plant hormone gibberellin (GA) is known to regulate elongating growth, seed germination, and the initiation of flower bud formation, and it has been postulated that GAs originally had functions in reproductive processes. Studies on the mechanism of induction of flowering by GA have been performed in *Arabidopsis* and other model plants. In coniferous trees, reproductive organ induction by GAs is known to occur, but there are few reports on the molecular mechanism in this system. To clarify the gene expression dynamics of the GA induction of the male strobilus in *Cryptomeria japonica*, we performed comprehensive gene expression analysis using a microarray. A GA-treated group and a nontreated group were allowed to set, and individual trees were sampled over a 6-week time course. A total of 881 genes exhibiting changed expression was identified. In the GA-treated group, genes related to 'stress response' and to 'cell wall' were initially enriched, and genes related to 'transcription' and 'transcription factor activity' were enriched at later stages. This analysis also clarified the dynamics of the expression of genes related to GA signaling transduction following GA treatment, permitting us to compare and contrast with the expression dynamics of genes implicated in signal transduction responses to other plant hormones. These results suggested that various plant hormones have complex influences on the male strobilus induction. Additionally, principal component analysis (PCA) using expression patterns of the genes that exhibited sequence similarity with flower bud or floral organ formation-related genes of *Arabidopsis* was performed. PCA suggested that gene expression leading to male strobilus formation in *C. japonica* became conspicuous within one week of GA treatment. Together, these findings help to clarify the evolution of the mechanism of induction of reproductive organs by GA.

Keywords: gibberellin; male strobilus induction; transcriptome; conifer; *Cryptomeria japonica*

1. Introduction

Gibberellins (GAs), a class of terpenoid plant hormones, regulate various important plant physiological processes, such as plant elongation, seed germination, and floral initiation [1,2]. The endogenous active GA_4 has been detected in the Lycopsida (*Selaginella moellendorffii*) but not in mosses (*Physcomitrella patens*) [3–5]. It is thought that GA signaling was acquired in the vascular plant

lineage after divergence of the bryophytes [5,6]. In ferns, GAs are involved in microspore formation and sex determination, and GAs are inferred to have originally functioned in reproductive processes [7,8].

Studies of the model plant *Arabidopsis thaliana* identified six flowering pathways, known as age, autonomous, vernalization, photoperiod, temperature, and GA [9–16]. GA-mediated floral transitions in angiosperms have been the subject of multiple studies performed in model plants, including *A. thaliana* [9,15,17,18].

Previous studies using *A. thaliana* reported several key observations. First, GAs are necessary for flowering under short day conditions [15,19,20]. Second, GAs promote the expression of *LEAFY* (*LFY*), a well-known floral meristem identity gene, via *cis*-elements (located within the *LFY* promoter) that can be bound by the GAMYB protein [18,21,22]. Third, *LFY* regulates GA levels through the activation of the GA catabolism gene and functions coordinately with *DELLA* (negative gibberellin-response regulator) and *SQUAMOSA PROMOTER BINDING PROTEIN-LIKE 9* (*SPL9*), thereby activating the *APETALA 1* (*AP1*) gene and inducing flowering [23].

In coniferous species, the dynamics of GAs and GA-related genes associated with the development of reproductive organs has been described [24–26]. Although physiological analyses have been performed to examine the effects of GA treatment [27], the mechanisms underlying the regulation of reproductive organ induction or differentiation by GAs remain unknown [28].

In many conifers, reproduction begins 5 to 10 years after planting [29]. However, in Japanese cedar (*Cryptomeria japonica* D. Don), the GA_3 treatment onto seedlings, even 1-year-old seedlings, facilitates male strobilus induction [30], indicating that the species possesses high reactivity to GAs. Therefore, *C. japonica* could be a useful model coniferous tree species for understanding the mechanism underlying the flowering induction by GAs.

The effects of GA_3 treatment on male strobilus induction in *C. japonica* have been investigated, particularly via phenotypic and physiological analyses [31]. The influence of the concentration and seasonal timing of GA_3 treatment on the induction of reproductive organs and the associated changes in carbohydrate and nitrogen content of the shoot have been studied [31]. It was shown that the male strobili were strongly induced by GA treatment in July, and the C–N ratio was significantly increased by GA treatment [31].

To clarify the molecular mechanism of male strobilus induction by GA_3 treatment in *C. japonica*, we conducted comprehensive gene expression analysis using the microarray method. GA_3-treated and non-treated individuals (as controls) were prepared and their current year shoots were sampled along a time course. The RNA from the shoot samples were subjected to the microarray analysis to obtain gene expression data. The extensive expression data obtained from the treated and non-treated samples at each time point were compared to determine when and which classes of gene transcripts were enriched following GA_3 treatment. Furthermore, we examined changes in the expression patterns of genes associated with the GA signaling pathway, other plant hormone signaling pathways, or flowering in other species, aiming at providing insights into GA functional mechanisms in male strobilus induction in *C. japonica*.

2. Materials and Methods

2.1. Plant Material and GA Treatment

Six individuals of three different plus-trees (plus-tree codes 1725, 840, and 1503) that had been planted in 1995 in Hitachi, Ibaraki, Japan (36°69 N, 140°69 E; elevation 52 m), were used for the gene expression analysis (Figure S1). One individual from each clone was designated as a GA-treated individual (1725_GA, 840_GA and 1503_GA) and subjected to the GA_3 treatment. The others were designated as non-treated individuals (1725_CT, 840_ CT and 1503_ CT). The GA_3 spraying was conducted at approximately 10:00 h on July 14, 2015. The branches of GA-treated individuals were sprayed with 100 ppm GA_3 (Kyowa-Hakko, Japan) solution. On July 13, 2015, approximately 3-cm-long shoots tips were sampled from the six individuals. This sampling period was designated as

−1 d (pre-dose). In the post-dose sampling periods, samples were collected after 3 h (14 July 2015), 1 day (1 d; 15 July 2015), 3 days (3 d; 17 July 2015), 1 week (1 w; 21 July 2015), 2 weeks (2 w; 27 July 2015), 4 weeks (4 w; August 11, 2015), and 6 weeks (6 w; 24 August 2015). Moreover, at each time point, samples were collected from the non-treated individuals (designated as CT; for example 1725_CT_3 h is the sample collected from the non-treated 1725 clone 3 h after the treatment period; Figure S1). All the samples, including the pre-dose ones, were collected at approximately 13:00 h. All 48 samples were stored at −80 °C until RNA extraction and analysis.

2.2. Extraction of Total RNA

Total RNA was extracted from each of the 48 samples using Plant RNeasy Mini Kits (QIAGEN, Hilden, Germany) according to the manufacturer's instructions, including on-column (i.e., prior to elution) DNase treatment with an RNase-Free DNase set (QIAGEN) according to the manufacturer's instructions. The quality of the total RNA in the samples was assessed using an Agilent 2100 Bioanalyzer and RNA 6000 Nano kit (Agilent Technologies, Mississauga, ON, Canada). The all samples exhibited an RNA integrity number (RIN) exceeding 7.7.

2.3. Microarray

The custom microarray was designed based on isotigs from next-generation sequencing (NGS) data as described in previous reports [32–34]. A set of 19,360 probes was selected and accommodated in the Agilent 8 × 60 K format (Agilent). In this format, 19,360 probes were accommodated in at least triplicate in our custom array, as described in a previous report (GEO accession: GPL21366, [35]). Gene annotations represent the top-scoring BLASTX hits using each sequence's predicted protein product as a query against The Arabidopsis Information Resource (TAIR; http://www.arabidopsis.org) Arabidopsis protein database TAIR10-pep-20101214 using the CLC Genomic Workbench version 4.1.1 software package (CLC bio, Aarhus, Denmark) as described in a previous report (Fukuda et al., 2018). Gene expression data were acquired using microarray analysis (Agilent Technologies). Total RNA (200 ng) from all 48 samples were amplified and labeled using a Low Input Quick-Amp Labeling Kit (Agilent Technologies). Hybridization and washing were performed according to the manufacturer's recommendations. Labeled and hybridized slides were scanned using a SureScan Microarray Scanner G4900DA (Agilent Technologies), and the dataset was trimmed using Agilent Feature Extraction Software 11.5.1.1 (Agilent Technologies). The data presented in this study have been deposited in NCBI's Gene Expression Omnibus and are accessible through GEO Series as accession number GSE120227.

2.4. Analyses of Gene Expression Patterns and Identification of Differentially Expressed Genes

Expression analysis of the genes was carried out using the Subio platform (Subio, Inc., Kagoshima, Japan, http://www.subio.jp) [36]. The raw signal data were converted to processed signal data using the following steps: (1) Global normalization was performed at the 75th percentile. (2) Log transformation was performed by converting the data to the $\log_2$ data. The genes used for analysis then were extracted using the following steps: (1) Among 19,360 isotigs, the isotigs that did not yield reliable data (i.e., those for which reliable measured values were not obtained with more than 91.7% of samples (in 44 out of 48 samples)) were excluded with filter glsWellAboveBG = 0 (QC1: 17,162 isotigs). (2) For all 48 samples, we excluded probes whose processed signal was in the range of −1 to 1 (QC2: 11,738 isotigs). Following these filtering steps, an average (mean) value was calculated for each of the three biological replicates (plus-tree codes 1725, 840, and 1503). Differentially expressed genes (DEGs) were detected via a two-step process, as follows: In Step 1, seven comparisons (DEG1 to 7) were performed, and gene groups whose expression levels differed by more than 2-fold and yielded p-values <0.05 (by two-tailed non-paired Student's t-test) were extracted using the Subio platform basic plug-in (Subio, Inc.). The comparisons (DEG1 to 7) were as follows (respectively): GA-treated (GA)_3 h vs. Control (CT)_3 h, GA_1 d vs. CT _1 d, GA_3 d vs. CT _3 d, GA_1 w vs. CT _1 w, GA_2 w vs. CT _2 w, GA_4 w vs. CT _4 w, and GA_6 w vs. CT _6 w. In Step 2, another seven comparisons were performed

against the Step-1 results. These Step-2 comparisons (DEG a to g) were as follows (respectively): GA_−1 d (Sample for subtracting genes specifically expressed in GA-treated individual) vs. DEG1, GA_−1 d vs. DEG2, GA_−1 d vs. DEG3, GA_−1 d vs. DEG4, GA_−1 d vs. DEG5, GA_−1 d vs. DEG6, and GA_−1 d vs. DEG7. A total of 881 DEGs were isolated from these comparisons. Tree clustering analyses of DEGs by Pearson correlation as a similarity measurement were performed using the Subio platform basic plug-in (Subio, Inc.) according to the corresponding instructional videos. Extraction of patterns of genes that had sequence similarity to plant hormone signal transduction genes of the KEGG pathway database (http://www.kegg.jp/kegg/pathway.html) were performed using the pathway edit tool of the Subio platform advanced plug-in (Subio Inc.) according to the corresponding instructional videos. Principal component analysis (PCA) of MADS-box genes in DEGs also was performed using the Subio platform basic plug-in according to the corresponding instructional videos.

2.5. Gene Ontology (GO) Analysis

GO analyses using the TAIR ID of the top hit for each DEG and for selected genes of our microarray (genes with E-values < 1E−5) were performed using the GO annotation search tool of TAIR in 8 April 2018. Enrichment analysis was carried out by comparing the GO analysis result of each cluster with the GO analysis result of all genes on our microarray. Enrichment analysis using the TAIR ID of the top hit for all DEGs with E-values < 1E−5 also was performed using DAVID Bioinformatics Resources 6.8 (https://david.ncifcrf.gov/) [37,38].

2.6. Real-Time PCR

To validate our microarray data, 16 samples were tested using the real-time PCR (RT-PCR) method. For RT-PCR analysis, RNA samples from each time point of GA-treated and nontreated plus-tree code 840 specimens were analyzed. A High-Capacity RNA-to-cDNA Kit (Thermo Fisher Scientific, Waltham, MA, USA) was used, and cDNA synthesis (20 µL) was performed using 450 ng of total RNA according to the kit's instruction manual. Primers, which were designed using Primer3Plus [39], were intended to have melting temperatures (Tm) between 60 °C and 65 °C, and to produce amplicons of 80 to 150 bp. Specific primer pairs are listed below. *AGAMOUS-like 9* (*AGL9*, *reCj28306:M—:isotig28158*): forward 5′-ATCTTCGTAAAAGGGAGACTTTGCT-3′, reverse 5′-GGGTCTGGAGTCTTGTTGAGTTG-3′); *UNUSUAL FLORAL ORGANS* (*UFO*, *reCj27181:—:isotig27033*): forward 5′-TGTGCTGTCTGTCGGAGAAC-3′, reverse 5′-CGATGACCTTGTATGTCTTGGTG-3′); *LEAFY 3* (*LFY3*, *reCj22786:—:isotig22638*): forward 5′-TGGCAAGTTTCTGCTGGATG-3′, reverse 5′-CATTTTCCCCTCGTTCTTTGTAG-3′); *PISTILLATA* (*PI*, *reCj29951:M—:isotig29803*): forward 5′-AAGAATGCCTCTGGAGGACG-3′, reverse 5′-TTCTTTGCTGCAAGCACAAGAGC-3′); and the endogenous control *Ubiquitin 10* (*UBQ10*): forward 5′-CGTTAAAGCCAAGATCCAGGACAA-3′, reverse 5′-TCCATCCTCAAGCTGTTTCCCA-3′) [34]. For each sample, triplicate RT-PCR assays were performed by using 1 µL of cDNA and Power SYBR Green PCR master mix (Thermo Fisher Scientific) according to the manufacturer's protocol. Amplification was carried out with a StepOnePlus system (Thermo Fisher Scientific). After an initial 10 min activation step at 95 °C, reactions were performed as 40 cycles at 95 °C for 15 s and 60 °C for 1 min, and a single fluorescence reading was obtained after each cycle (immediately following the annealing/elongation step at 60 °C). Preliminary RT-PCR assays were performed to evaluate primer pair efficiency. A melting curve analysis was performed at the end of cycling to ensure that a single product had been amplified. For relative quantification and comparisons, we used the delta-delta-Ct method [40] with the *UBQ10* transcript as the internal normalization control.

3. Results

3.1. DEG Enrichment in Response to GA_3 Treatment

Male strobili of *C. japonica* were induced by GA_3 spraying onto the shoots. We collected 48 samples using three different plus-trees as biological repeats; one individual in each plus-tree was treated with GA or non-treated individual (CT), and samples were collected at each of the eight time points (1 pre-dose, 7 post-dose up to 6 w). Male strobili are formed at the axil of shoots. Male strobili were phenotypically confirmed on the shoots of treated individuals on August 24, 2015 (6 w; Figure 1). The differentially expressed genes (DEGs) were extracted to permit assessment of the transcriptional response to GA_3 treatment. Using the Subio platform tree clustering tool, the resulting 881 DEGs were sorted into several clusters according to their expression profiles (Pearson correlation, Figure 2), and were organized into three primary clusters (Clusters D, U1, and U2) (Figure 2, Table S1). Cluster D comprised of genes that were downregulated in GA-treated samples (379 DEGs) compared with those in CT samples. Conversely, the remaining two clusters U1 and U2 comprised of genes that were upregulated in the GA-treated samples (104 DEGs and 398 DEGs, respectively) compared with those in CT samples. Cluster U1 was characterized by genes that were upregulated at earlier time points following the GA_3 treatment, whereas cluster U2 was characterized by genes that were gradually upregulated as the time course progressed.

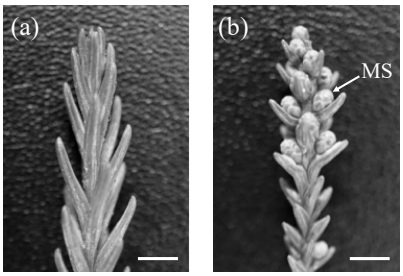

Figure 1. Morphology of the shoot top of *Cryptomeria japonica*: (**a**) nontreated control sample at 6 weeks (CT_6 w); (**b**) GA3-treated sample at 6 weeks (GA_6 w). Male strobili (MS; indicated by arrow) are formed at the axil of the shoot.

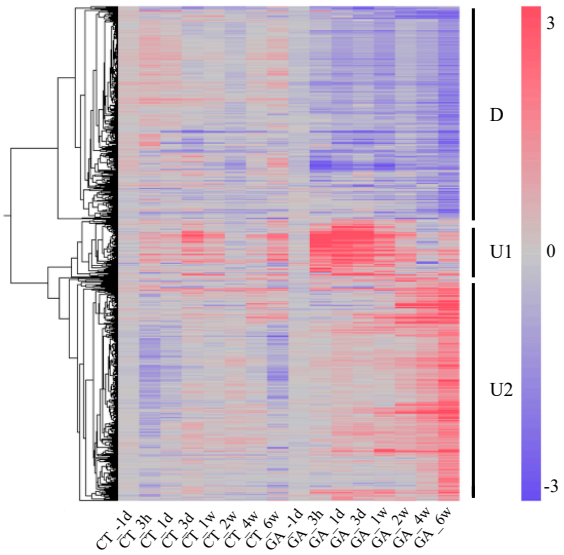

Figure 2. Tree clustering analysis of 881 DEGs. D, U1, and U2 on the right indicate three different clusters of differentially expressed genes (DEGs) used for further analysis. CT_−1 d, CT_3 h, CT_1 d, CT_3 d, CT_1 w, CT_2 w, CT_4 w, CT_6 w, GA_−1 d, GA_3 h, GA_1 d, GA_3 d, GA_1 w, GA_2 w, GA_4 w, and GA_6 w are sample names.

3.2. Functional Analysis of DEGs

To categorize the genes included in each cluster, we selected the annotated DEGs with low E-values (<1E−5) and performed GO enrichment analysis (Figure 3). Our data suggested that 'response to stress', 'response to abiotic or biotic stimulus' (Biological Process), 'cell wall', 'extracellular' (Cellular Component), and 'kinase activity' (Molecular Function) -related genes were enriched in Cluster U1 (90 DEGs); 'transcription, DNA-dependent' (Biological Process), 'cell wall', 'extracellular' (Cellular Component), 'transcription factor activity', and 'nucleic acid binding' (Molecular Function) -related genes were enriched in Cluster U2 (336 DEGs); and 'electron transport or energy pathway' (Biological Process), 'plastid' (Cellular Component), and 'receptor binding or activity' (Molecular Function) -related genes were enriched in Cluster D (324 DEGs). Enrichment analysis, performed using DAVID, yielded similar patterns (Table S2).

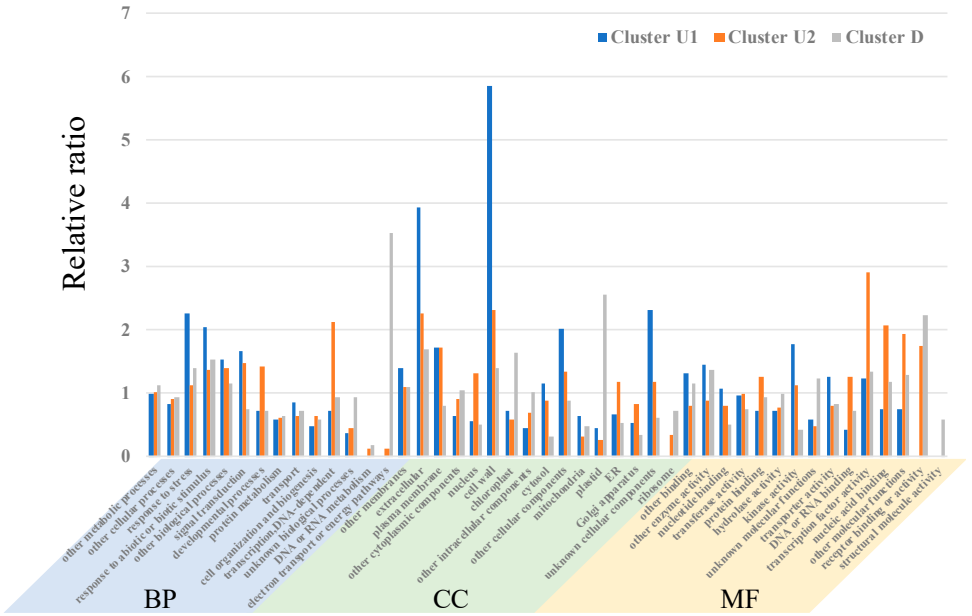

Figure 3. Gene ontology (GO) categories of DEGs that encoded proteins with sequence similarity (E-value <1E−5) to proteins in the TAIR database. The longitudinal axis shows the relative ratio of the genes of Cluster U1 (blue), U2 (orange), and D (gray) against GO analysis results for all genes on the custom microarray (GEO accession: GPL21366). BP: biological process, CC: cellular component, MF: molecular function.

3.3. Expression Patterns of GA Signaling Pathway Genes

To clarify the expression patterns of GA signaling pathway-related genes following the GA_3 treatment of *C. japonica*, the expression patterns of genes exhibiting high sequence similarity (E-value <1E−5) with plant hormone signal transduction genes (KEGG Pathway Database) were extracted using the Subio Platform pathway edit tool (Figure 4, Table 1). Among the remaining genes, *reCj11694* exhibiting high sequence similarity to *RGA-LIKE 2* (*RGL2*), which encodes the DELLA protein, was observed in Cluster U2, whereas *reCj34040* and *reCj28549* exhibiting high sequence similarity to *SLEEPY1* (*SLY1*), the rice ortholog of *GID2* [41], were observed in Cluster D. Specifically, the *reCj11694* transcript (encoding a DELLA-like protein) accumulated gradually in the GA-treated samples (Figure 4, Table 1), whereas the levels of the *reCj34040* and *reCj28549* transcripts (encoding SLY1-like proteins) decreased in the GA-treated samples (Figure 4, Table 1). Other potentially relevant genes included *reCj21012* [encoding a protein with sequence similarity to GA INSENSITIVE DWARF 1A (GID1A), a GA receptor], *reCj28386* and *reCj11695* (encoding proteins with sequence similarity to RGL2), *reCj09118* [encoding a protein with sequence similarity to GIBBERELLIC ACID INSENSITIVE (GAI), a DELLA protein], *reCj31917* and *reCj15916* (encoding proteins with sequence similarity to SLY1), and *reCj23186*

[encoding a protein with sequence similarity to PHYTOCHROME INTERACTING FACTOR 3 (PIF3)]. These members of the QC1 gene pool showed relatively constant expression with little fluctuation in their expression levels following GA_3 treatment (Figure S2).

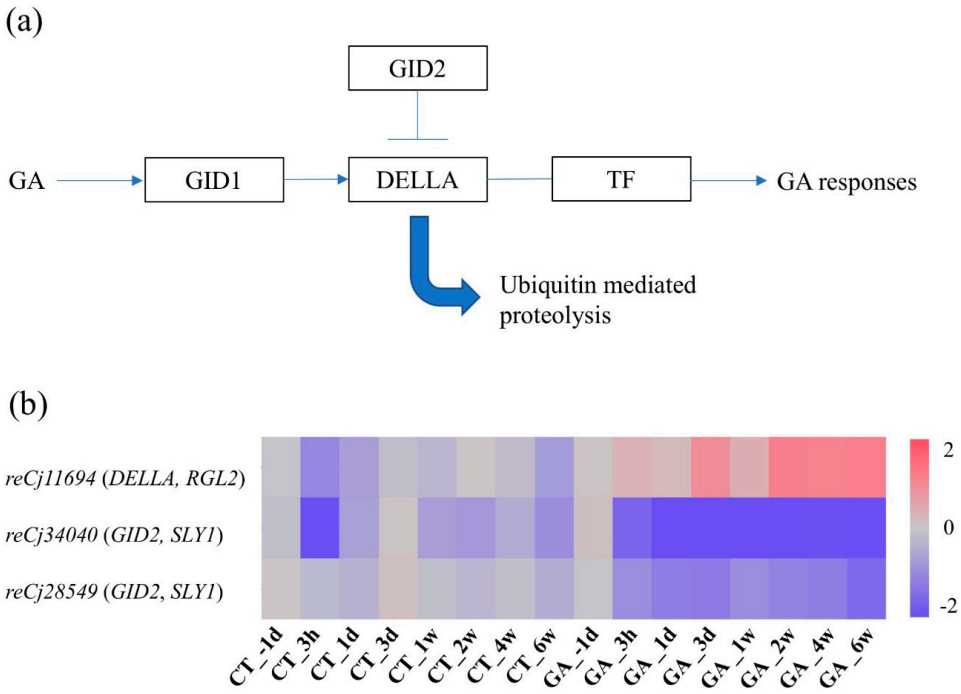

Figure 4. The DEG analysis associated with gibberellin (GA) signal transduction. (**a**) GA signal transduction pathway modified KEGG plant hormone signal transduction reference pathway (https://www.genome.jp/kegg-bin/show_pathway?map04075). GID1: GA INSENSITIVE DWARF 1, DELLA: DELLA protein, GID2: GIBBERELLIN INSENSITIVE DWARF 2, TF: transcription factor; (**b**) The heat-map of DEGs associated with GA signal transduction of each sample. The relative expression values were $\log_2$ transformed. Red indicates high expression; blue indicates low expression. CT_−1 d, CT_3 h, CT_1 d, CT_3 d, CT_1 w, CT_2 w, CT_4 w, CT_6 w, GA_−1 d, GA_3 h, GA_1 d, GA_3 d, GA_1 w, GA_2 w, GA_4 w, and GA_6 w are sample names. Details of these genes are provided in Table 1.

Table 1. The DEGs associated with plant hormone signaling pathways after GA_3 treatment.

SEQ_ID	Short SEQ_ID	Arabi_ID	Symbol	Description	E-Value
reCj11694:-S–:isotig11549	reCj11694	AT3G03450	RGL2	RGA-like_2	7.86E−56
reCj34040:—-:isotig33892	reCj34040	AT4G24210	SLY1	F-box_family_protein	6.88E−24
reCj28549:-SWR:isotig28401	reCj28549	AT4G24210	SLY1	F-box_family_protein	1.02E−24
reCj31635:—-:isotig31487	reCj31635	AT2G21220	SAUR12	SAUR-like_auxin-responsive_protein_family	7.47E−30
reCj30256:-S–:isotig30108	reCj30256	AT5G20810	SAUR70	SAUR-like_auxin-responsive_protein_family	6.82E−26
reCj27704:-SWR:isotig27556	reCj27704	AT4G14550	IAA14	SLR_indole − 3-acetic_acid_inducible_14	9.46E−76
reCj19503:M–R:isotig19355	reCj19503	AT1G28130	GH3.17	Auxin-responsive_GH3_family_protein	0
reCj19606:M–R:isotig19458	reCj19606	AT5G54510	GH3.6	Auxin-responsive_GH3_family_protein	0
reCj27651:–WR:isotig27503	reCj27651	AT3G57040	ARR9	ATRR4_response_regulator_9	9.29E−39
reCj26644:–W-:isotig26496	reCj26644	AT2G29380	HAI3	highly_ABA-induced_PP2C_gene_3	1.19E−74
reCj25311:–WR:isotig25163	reCj25311	AT2G29380	HAI3	highly_ABA-induced_PP2C_gene_3	2.06E−94
reCj12520:MS-R:isotig12375	reCj12520	AT5G20900	JAZ12	jasmonate-zim-domain_protein_12	2.83E−16
reCj27869:-SWR:isotig27721	reCj27869	AT1G19180	JAZ1	jasmonate-zim-domain_protein_1	1.48E−15
reCj27238:-SWR:isotig27090	reCj27238	AT1G70700	JAZ9	TIFY_domain/Divergent_CCT_motif_family_protein	3.15E−17
reCj23299:MSWR:isotig23151	reCj23299	AT3G50070	CYCD3	CYCLIN_D3;3	2.35E−62
reCj28941:—-:isotig28793	reCj28941	AT5G67260	CYCD3	CYCLIN_D3;2	9.03E−40
reCj32790:—-:isotig32642	reCj32790	AT4G33720	PR1	CAP_(Cysteine-rich_secretory_proteins,_Antigen_5, _and_Pathogenesis-related_1_protein)_superfamily_protein	8.24E−62
reCj20357:–W-:isotig20209	reCj20357	AT2G41370	BOP2	Ankyrin_repeat_family_protein_/_BTB/POZ _domain-containing_protein	1.11E−158
reCj31882:-S–:isotig31734	reCj31882	AT4G33720	PR1	CAP_(Cysteine-rich_secretory_proteins,_Antigen_5, _and_Pathogenesis-related_1_protein)_superfamily_protein	9.89E−63
reCj31173:—R:isotig31025	reCj31173	AT4G33720	PR1	CAP_(Cysteine-rich_secretory_proteins,_Antigen_5, _and_Pathogenesis-related_1_protein)_superfamily_protein	5.87E−62

3.4. Expression Patterns of Genes Encoding Components of Other Plant Hormone Signaling Pathways

The expression patterns of genes encoding components of other plant hormone signaling pathways were also examined. The 17 genes exhibiting high sequence similarity to those listed in the plant hormone signal transduction pathway in the KEGG Pathway Database were extracted from the DEGs identified in the present study (Figure 5, Table 1). Five of the extracted DEGs corresponded to components of the auxin signal transduction pathway. Specifically, the expression of *reCj31635* and *reCj30256*, which encode proteins with sequence similarity to members of the auxin-responsive SAUR protein family, was repressed compared to expression of the respective genes in the non-treated samples. On the other hand, the expression of *reCj27704*, which encodes a protein with sequence similarity to IAA14 (a negative regulator of *Auxin response factor 7*), was upregulated at 4 weeks after GA_3 treatment (GA_4 w). The expression of *reCj19503* and *reCj19606*, which encode proteins with sequence similarity to GH3 (indole−3-acetic acid (IAA) -amido synthase), was upregulated at GA_3 d and GA_1 w, respectively. The *reCj26644* and *reCj25311* were extracted from the abscisic acid signal transduction pathway based on sequence similarity to *Highly-ABA induced PPC2 gene 3* (*HAI3*). The expression of these genes was upregulated at GA_1 w and GA_4 w, respectively. The *reCj12520*, *reCj27869*, and *reCj27238* were extracted from the jasmonic acid signal transduction pathway based on sequence similarity to *JAZ*, which encodes a negative regulator. The expression of these genes was upregulated as follows after GA_3 treatment: *reCj12520* gradually increased, *reCj27869* from GA_3 h, and *reCj27238* at GA_1 w (intensively) and at GA_6 w. *reCj20357*, *reCj32790*, *reCj31882*, and *reCj31173* were extracted from the salicylic acid signal transduction pathway based on the sequence similarity of *reCj20357* to *BLADE ON PETIOLE2* (*BOP2*) (*NONEXPRESSER OF PR GENES 1* (*NPR1*)-like; encoding a member of the ankyrin repeat family) and of *reCj32790*, *reCj31882*, and *reCj31173* to *pathogenesis-related protein 1* (*PRI*). The *reCj20357* exhibited a gradual increase of expression starting from GA_3 h, whereas *reCj32790* was gradually downregulated; the expression of both *reCj31882* and *reCj31173* was strongly upregulated after GA_1 d.

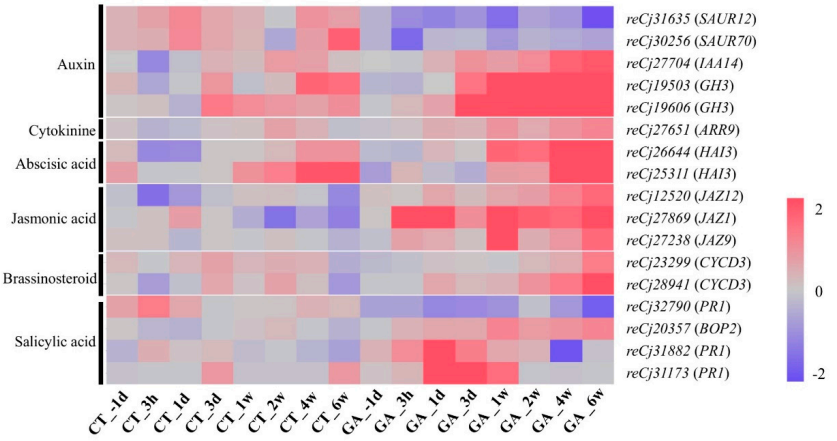

Figure 5. The heat map analysis associated with plant hormone signal transduction pathways without GA. The relative expression values were $\log_2$ transformed. Red indicates high expression; blue indicates low expression. CT_−1 d, CT_3 h, CT_1 d, CT_3 d, CT_1 w, CT_2 w, CT_4 w, CT_6 w, GA_−1 d, GA_3 h, GA_1 d, GA_3 d, GA_1 w, GA_2 w, GA_4 w, and GA_6 w are sample names. Details of these genes are provided in Table 1.

3.5. Expression Patterns of MADS-Box Genes

MADS-box genes are well known as floral homeotic genes [42,43]. To clarify changes in the expression patterns of MADS-box genes after GA_3 treatment in *C. japonica*, 18 DEGs encoding MADS-box proteins (E-value <1E−5) were extracted (Figure 6, Table 2). These genes were divided into two classes based on the associated expression patterns. The first class consisted of genes whose expression increased gradually following the GA_3 treatment, and included *reCj29105*, *reCj27161*,

reCj32389, *reCj31907*, *reCj28306*, *reCj31827*, *reCj29951*, *reCj33073*, *reCj30226*, *reCj30596*, *reCj17268*, and *reCj25811*. The second class consisted of genes whose expression gradually decreased following the GA_3 treatment such as *reCj271510*, *reCj15424*, *reCj29820*, *reCj30835*, *reCj15467*, and *reCj29690*. Based on sequence similarity, the upregulated genes included the following: *reCj31097*, *reCj33073*, and *reCj30226* resembled *AGL6* (which encodes a protein that activates the florigen-encoding locus *FLOWERING LOCUS T* (*FT*) and downregulates the floral repressor-encoding *FLC/MAF*-clade genes, including *FLOWERING LOCUS C* (*FLC*)); *reCj29105* and *reCj28306* resembled *SEPALLATA 1* (*SEP1*) and *SEPALLATA 3* (*SEP3*), respectively, known floral organ identity genes; *reCj31827*, *reCj30596*, *reCj27161*, and *reCj29951* resembled *PISTILLATA* (*PI*), a known floral organ identity gene; and *reCj32389*, *reCj17268*, and *reCj25811* resembled *AGL16*, *AGL15* and *SHP1*, respectively. On the other hand, the downregulated genes included the following: *reCj15424*, *reCj29690*, and *reCj15467* had sequence similarity to *FRUITFULL* (*FUL*), which is downregulated by *APETALA 1* (*AP1*); *reCj27510* had sequence similarity to *AGL22*, a known floral repressor; *reCj29820* had sequence similarity to *AGL20*, which is known to act with *AGL24* to promote flowering and floral meristem identity; and *reCj30835* had sequence similarity to *AGL19*, a known floral activator. Then PCA analysis was carried out using the expression patterns of these 18 genes to estimate the transition from vegetative growth phase to reproductive growth phase (Figure 7). The variance contribution of first and second components of PCA was 94.3% and 1.9%, respectively. Large temporal change of expression patterns was observed in the direction along with the first principal component. After 1 week, divergence in the expression of these genes was observed between the GA-treated and CT samples, and it became evident with the time course.

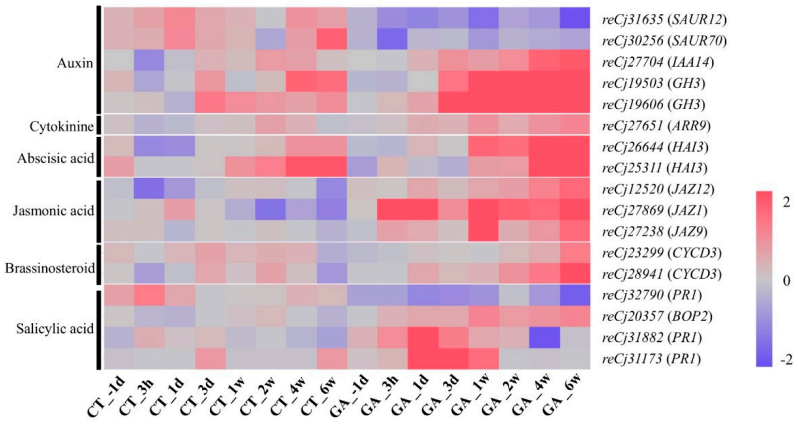

Figure 6. The heat map analysis associated with MADS-box genes. The relative expression values were $\log_2$ transformed. Red indicates high expression; blue indicates low expression. CT_−1 d, CT_3 h, CT_1 d, CT_3 d, CT_1 w, CT_2 w, CT_4 w, CT_6 w, GA_−1 d, GA_3 h, GA_1 d, GA_3 d, GA_1 w, GA_2 w, GA_4 w, and GA_6 w are sample names. Details of these genes are provided in Table 2.

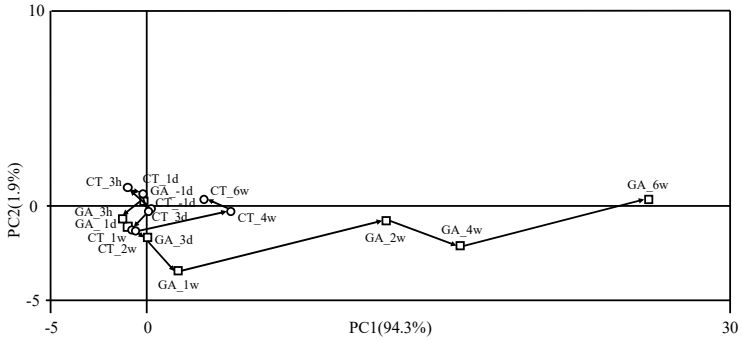

Figure 7. Principal component analysis of all samples for 18 DEGs, including the MADS-box genes listed in Table 2; expression patterns were described in Figure 7. Open circles indicate GA-nontreated control samples. Open squares indicate GA-treated samples.

Table 2. The DEGs associated with MADS-box genes after GA_3 treatment.

SEQ_ID	Short SEQ_ID	Arabi_ID	Symbol	Description	E-Value
reCj29105:-S–:isotig28957	reCj29105	AT5G15800	SEP1, AGL2	K-box_region_and_MADS-box_transcription_factor_family_protein	5.59E−30
reCj27161:MS–:isotig27013	reCj27161	AT5G20240	PI	K-box_region_and_MADS-box_transcription_factor_family_protein	1.63E−48
reCj32389:M—:isotig32241	reCj32389	AT3G57230	AGL16	AGAMOUS-like_16	4.66E−24
reCj31097:M—:isotig30949	reCj31097	AT2G45650	AGL6	AGAMOUS-like_6	8.94E−33
reCj28306:M—:isotig28158	reCj28306	AT1G24260	SEP3, AGL9	K-box_region_and_MADS-box_transcription_factor_family_protein	4.47E−54
reCj31827:M—:isotig31679	reCj31827	AT5G20240	PI	K-box_region_and_MADS-box_transcription_factor_family_protein	2.06E−33
reCj29951:M—:isotig29803	reCj29951	AT5G20240	PI	K-box_region_and_MADS-box_transcription_factor_family_protein	1.35E−31
reCj33073:M—:isotig32925	reCj33073	AT2G45650	AGL6	AGAMOUS-like_6	1.51E−21
reCj30226:M—:isotig30078	reCj30226	AT2G45650	AGL6	AGAMOUS-like_6	5.87E−33
reCj30596:M—:isotig30448	reCj30596	AT5G20240	PI	K-box_region_and_MADS-box_transcription_factor_family_protein	2.00E−36
reCj17268:—-:isotig17123	reCj17268	AT5G13790	AGL15	AGAMOUS-like_15	3.50E−18
reCj25811:MS–:isotig25663	reCj25811	AT3G58780	SHP1	K-box_region_and_MADS-box_transcription_factor_family_protein	4.57E−47
reCj27510:-SW-:isotig27362	reCj27510	AT2G22540	AGL22	K-box_region_and_MADS-box_transcription_factor_family_protein	2.05E−40
reCj15424:-SW-:isotig15279	reCj15424	AT5G60910	AGL8	AGAMOUS-like_8	7.64E−34
reCj29820:–W-:isotig29672	reCj29820	AT2G45660	AGL20	AGAMOUS-like_20	1.88E−39
reCj30835:—-:isotig30687	reCj30835	AT4G22950	AGL19	AGAMOUS-like_19	9.09E−25
reCj15467:—-:isotig15322	reCj15467	AT5G60910	AGL8	AGAMOUS-like_8	4.67E−34
reCj29690:-SW-:isotig29542	reCj29690	AT5G60910	AGL8	AGAMOUS-like_8	4.52E−37

3.6. Validation Using Real-Time PCR

To validate our microarray data, 64 test reactions (4 DEGs, in both GA-treated and -nontreated samples, from each of the eight time points) were tested by RT-PCR (Figure 8). Its result demonstrated that the microarray data obtained were highly reproducible and reliable.

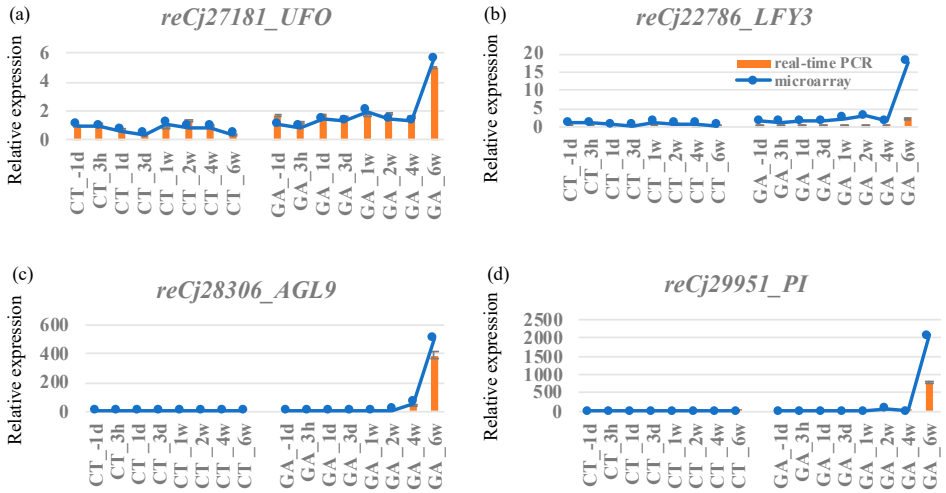

Figure 8. Real-time PCR validation of DEGs data. Bar graphs show relative expression from real-time PCR and line graphs show raw data signals from microarray analysis. Data are presented as mean + standard deviation (n = 3). (**a**) *reCj27181_UFO*, (**b**) *reCj22786_LFY3*, (**c**) *reCj28306_AGL9*, (**d**) *reCj29951_PI*. CT_−1 d, CT_3 h, CT_1 d, CT_3 d, CT_1 w, CT_2 w, CT_4 w, CT_6 w, GA_−1 d, GA_3 h, GA_1 d, GA_3 d, GA_1 w, GA_2 w, GA_4 w, and GA_6 w are sample names.

4. Discussion

4.1. Comprehensive Gene Expression Dynamics Following GA_3 Treatment

Our research clarified changes in gene expression patterns during male strobilus induction following GA_3 treatment. We used the microarray method for comparative analyses of gene expression patterns between GA-treated and non-treated samples.

Overall, the analyses identified 881 DEGs that showed >2-fold changes in expression for a given time point (when comparing GA-treated samples to nontreated samples) or when comparing expression before and after GA_3 treatment. Cluster analyses revealed that these 881 DEGs were grouped into three clusters (U1, U2, and D) depending on up- or down-regulation along the time course. In the following paragraphs, based on the expression patterns of the DEGs, we discussed their potential role in the mechanism of GA-induced male strobilus formation or other functions in *C. japonica*.

4.2. The Expression of GA Signal Transduction-Related Genes

Genes that had sequence similarity with GA signal transduction-related genes were detected among the DEGs. A *DELLA*-like gene (*reCj11694*) was upregulated by GA_3 treatment, whereas *SLY1*-like genes (*reCj34040* and *reCj28549*) were downregulated by GA_3 treatment (Figure 4). Detailed research on the molecular mechanism of GA signal transduction has been carried out in model plants like *Oryza sativa* and *A. thaliana*. In those systems, GAs bind to the GA receptor (GID1), enabling GID1 to interact with DELLA repressor proteins, which are negative regulators of GA signaling [44–46]. DELLA interacts with transcription factors, either impairing transcription factor function (by inhibiting factor ability to bind DNA) or enhancing DNA binding (by acting as a transcriptional coactivator) [47–50]. These GA-induced GID1-DELLA interactions lead to the degradation of DELLA repressors through the Skp, Cullin, F-box complex [3,46,51]. Concordantly with the results found in the present study, the upregulation of *DELLA*-like genes in response to GA treatment has been reported in grape and jatropha,

suggesting the possibility that the upregulation of *DELLA* is the result of feedback regulation via GA signaling [52,53]. Regulation by a GA feedback mechanism may be also able to apply in *C. japonica*. Validation of this hypothesis will require further analysis, including determination of quantitative changes of DELLA protein levels in response to GA treatment.

4.3. Expression of Male Strobilus Formation-Related Genes and the Growth Phase Transition from Vegetative to Reproductive Phase by GA Treatment

In *A. thaliana*, GAs promote expression of both *SUPPRESSOR OF OVEREXPRESSION OF CO1* (*SOC1*) and *LFY* directly, and regulate the expression of *SOC1* and *LFY* indirectly (via *GAMYB*) [15]. In the present study, DEGs also included various flower bud formation-related genes, including genes with higher sequence similarity to *LFY*. These DEGs also consisted of genes with high homology to *SHORT VEGETATIVE PHASE* (*SVP*) and *FUL*, genes that are known to be floral meristem identity genes. *SVP* encodes a floral repressor [54] and, like *FUL*, is negatively regulated by *AP1*, which is also a floral meristem identity gene [55,56]. Expression of these genes in *C. japonica* was suppressed during male strobilus formation (Figure 6). In *C. japonica*, these genes may function as suppressors of male strobilus formation. DEGs identified in the present study also included genes with sequence similarity to *SEP1*, *SEP3*, and *PI*, all of which are known as floral organ identity genes [42]. These DEGs were activated during male strobilus formation in *C. japonica* (Figure 6). In addition, activation of genes whose expression in flower buds and floral organs has been reported in another species was observed during male strobilus formation in *C. japonica*. Notably, Tsubomura et al. [57] comprehensively analyzed the expression of genes in the male strobilus and pollen development processes in *C. japonica*, revealing the expression patterns of genes associated with these developmental stages. Those authors observed that these *C. japonica* genes showed similarities in both sequence and expression pattern compared to the corresponding *A. thaliana* genes employed in tapetum development, indicating that these genes play an important role in processes that are fundamental to the maintenance of reproduction in the respective plant species. In the present study, we clarified the comprehensive gene expression dynamics of male strobilus induction, at an earlier stage than the morphology of male strobilus characterized by Tsubomura et al. [57]. Despite structural differences in the development of reproductive organs in *C. japonica* and *A. thaliana*, the expression patterns of relevant genes in these two species were similar, suggesting that the function of these genes have been preserved during evolution. In the present study, based on the sequence similarity to *A. thaliana* MADS-box genes, the corresponding *C. japonica* genes were extracted from the DEGs and annotated. Based on the expression pattern of these *C. japonica* genes, we inferred the transitional timing from the vegetative phase to the reproductive phase in male strobilus formation process as to be 1 week after GA_3 treatment because the divergence in expression dynamics along the first principal component between the GA-treated and -nontreated samples was exhibited at 1 week after the GA_3 treatment and increased with the time course (Figure 7).

4.4. Crosstalk with Auxin Signal Transduction During Male Strobilus Formation

Various studies have reported on possible crosstalk between the pathways regulated by GA and by other plant hormones [58–60]. In *A. thaliana*, it has been reported that auxin signal transduction is involved in the activation of the *LFY* gene; expression of the *LFY* gene is activated by the addition of auxin, resulting in flower bud formation [61,62]. Among the DEGs isolated in the present study, five kinds of genes showing sequence similarity to genes of the auxin signal transduction pathway were identified. Notably, *reCj31635* and *reCj30256*, which encode proteins with sequence similarity to SAURs (members of an auxin-responsive family of proteins) were downregulated in GA-treated samples compared to nontreated samples. On the other hand, *reCj27704*, a gene with sequence similarity to *IAA14* [a negative regulator of *Auxin response factor 7* [63]] was upregulated in GA-treated samples compared to nontreated samples. Moreover, *reCj19503* and *reCj19606*, which encode proteins with sequence similarity to GH3 (IAA-amido synthetase) also were upregulated in GA-treated samples compared to non-treated samples. These results suggested that the auxin signaling system may be

suppressed upon GA_3 treatment, an observation that would be consistent with results reported in jatropha [53]. In *C. japonica*, it was reported that auxin alone does not yield male strobilus induction, although the combination of auxin and GA was reported to increase the ratio of female cones [31].

4.5. Growth Control by GA Treatment

Enrichment analysis suggested that Cluster U1 contained many genes related to the response to stress, response to abiotic or biotic stimulus, extracellular, cell wall, other cellular components and unknown cellular components (Figure 3). Hou et al. [49] analyzed the genes targeted by DELLA during flower development in *A. thaliana* and reported that cell wall proteins were among the genes downregulated by RGA. GA has been hypothesized to have roles in both growth regulation and reproductive control. Notably, it has been reported that the GA_3 treatment promoted principal axis elongation and suppressed lateral branch elongation in *C. japonica* [64]. The accumulation of the transcripts of cell wall-related genes and cellular component genes, including WAKs-like genes (*reCj12226*, *reCj12227*, and *reCj32277*; Table S1; [65]), as revealed in the present study, might indicate the role of GA in growth control.

4.6. Senescence-Like Gene Expression Patterns Following GA Treatment

Enrichment analysis showed that Cluster D contained genes related to electron transport or energy pathway (related to photosystem I or photosystem II, etc.), plastids, chloroplasts, and receptor binding or activity (Figure 3, Table S2). This result suggested a decrease in the expression of photosynthesis-related genes. The decreased expression of photosynthesis-related genes is known as a leaf senescence-related phenomenon [66]. The *A. thaliana* NAC and WRKY53 proteins are known as transcription factors that play important roles in the process of senescence [67,68]. Among the DEGs identified in the present work, a gene (*reCj22492*) with sequence similarity to the *A. thaliana WIP5* gene (a putative target of *WRKY53* [68]) was detected within Cluster U2, indicating that this *C. japonica* gene is upregulated during the male strobilus formation process (Figure S3). In addition, plant hormones have been reported to participate in leaf senescence [69–71]. The abscisic acid signal transduction gene *SAG113* (*PP2C*) has been shown to be induced in the process of senescence [71,72]. The DEGs of *C. japonica* included two genes (*reCj26644* and *reCj25311*) with sequence similarity to *PP2C*; expression patterns placed these genes in Cluster U2, such that expression was increased during male strobilus formation (Figure 5). The U1 cluster of DEGs was enriched for genes annotated to be involved in response to stress and response to abiotic or biotic stimulus (Figure 3). These observations together suggested that the phenomena of senescence and stress response may overlap with each other and/or with the response to GA treatment in *C. japonica*; further study will be needed to clarify these inferences.

5. Conclusions

In conclusion, gene expression analysis facilitated better understanding of the molecular dynamics of the induction by GA_3 treatment of male strobilus formation in *C. japonica*. Our study identified various *C. japonica* genes with sequence similarity to genes implicated in GA signaling in other plant species. Our results revealed that the dynamics of gene expression for male strobilus formation became conspicuous from seven days after GA_3 treatment. In addition, we were able to capture the behavior of genes that may explain other phenomena resulting from GA_3 treatment. These data are expected to permit clarification of the molecular mechanism of the induction by GA_3 treatment of male strobilus formation in *C. japonica*, providing detailed information at the protein and metabolite levels. This information for *C. japonica*, a coniferous species, might provide new knowledge of the basic mechanism whereby evolution acquired a GA-regulated pathway for use in the induction of plant reproductive organs.

Supplementary Materials: The following are available online at http://www.mdpi.com/1999-4907/11/6/633/s1, Figure S1: Sampling scheme of this study, Figure S2: The heat map analysis associated with GA signal transduction pathways, Figure S3: The heat map of *reCj22492*, Table S1: The list of DEGs, Table S2: Results of enrichment analysis using DAVID.

Author Contributions: K.M. and M.K. conceived and designed the experiments; K.M. and M.K. performed the experiments; M.K. and K.M. analyzed the data; M.T. (Miyoko Tsubomura), Y.T., M.N. and T.H. contributed EST data/materials/analysis tools; M.K. wrote the manuscript; K.M., M.T. (Miyoko Tsubomura) and M.T. (Makoto Takahashi) revised the manuscript. All authors have read and agreed to the published version of the manuscript.

Funding: The present study is part of the project on 'Development of adaptation techniques to the climate change in the sectors of agriculture, forestry, and fisheries' supported by the Ministry of Agriculture, Forestry and Fisheries, Japan.

Acknowledgments: We are grateful to Hiroshi Hoshi (FTBC, FFPRI) for his well coordination of the research project.

Conflicts of Interest: The authors declare that the research was conducted in the absence of any commercial or financial relationships that could be construed as a potential conflict of interest.

References

1. Richards, D.E.; King, K.E.; Ait-Ali, T.; Harberd, N.P. How gibberellin regulates plant growth and development: A molecular genetic analysis of gibberellin signaling. *Annu. Rev. Plant Physiol. Plant Mol. Biol.* **2001**, *52*, 67–88. [CrossRef] [PubMed]
2. Sun, T.-P.; Gubler, F. Molecular Mechanism of Gibberellin Signaling in Plants. *Annu. Rev. Plant Boil.* **2004**, *55*, 197–223. [CrossRef]
3. Hirano, K.; Nakajima, M.; Asano, K.; Nishiyama, T.; Sakakibara, H.; Kojima, M.; Katoh, E.; Xiang, H.; Tanahashi, T.; Hasebe, M.; et al. The GID1-Mediated Gibberellin Perception Mechanism Is Conserved in the Lycophyte *Selaginella moellendorffii* but Not in the Bryophyte *Physcomitrella patens*. *Plant Cell* **2007**, *19*, 3058–3079. [CrossRef] [PubMed]
4. Vandenbussche, F.; Fierro, A.C.; Wiedemann, G.; Reski, R.; Van Der Straeten, D. Evolutionary conservation of plant gibberellin signalling pathway components. *BMC Plant Boil.* **2007**, *7*, 65. [CrossRef] [PubMed]
5. Hayashi, K.-I.; Horie, K.; Hiwatashi, Y.; Kawaide, H.; Yamaguchi, S.; Hanada, A.; Nakashima, T.; Nakajima, M.; Mander, L.N.; Yamane, H.; et al. Endogenous diterpenes derived from *ent*-kaurene, a common gibberellin precursor, regulate protonema differentiation of the moss *Physcomitrella patens*. *Plant Physiol.* **2010**, *153*, 1085–1097. [CrossRef] [PubMed]
6. Hirano, K.; Ueguchi-Tanaka, M.; Matsuoka, M. GID1-mediated gibberellin signaling in plants. *Trends Plant Sci.* **2008**, *13*, 192–199. [CrossRef] [PubMed]
7. Aya, K.; Hiwatashi, Y.; Kojima, M.; Sakakibara, H.; Ueguchi-Tanaka, M.; Hasebe, M.; Matsuoka, M. The Gibberellin perception system evolved to regulate a pre-existing GAMYB-mediated system during land plant evolution. *Nat. Commun.* **2011**, *2*, 544. [CrossRef]
8. Tanaka, J.; Yano, K.; Aya, K.; Hirano, K.; Takehara, S.; Koketsu, E.; Ordonio, R.L.; Park, S.-H.; Nakajima, M.; Ueguchi-Tanaka, M.; et al. Antheridiogen determines sex in ferns via a spatiotemporally split gibberellin synthesis pathway. *Science* **2014**, *346*, 469–473. [CrossRef]
9. Conti, L. Hormonal control of the floral transition: Can one catch them all? *Dev. Boil.* **2017**, *430*, 288–301. [CrossRef]
10. Mouradov, A.; Cremer, F.; Coupland, G. Control of flowering time: Interacting pathways as a basis for diversity. *Plant Cell* **2002**, *14*. [CrossRef]
11. Simpson, G.G.; Dean, C. *Arabidopsis*, the Rosetta Stone of Flowering Time? *Science* **2002**, *296*, 285–289. [CrossRef] [PubMed]
12. Andrés, F.; Coupland, G.; Andr, F. The genetic basis of flowering responses to seasonal cues. *Nat. Rev. Genet.* **2012**, *13*, 627–639. [CrossRef] [PubMed]
13. Bäurle, I.; Dean, C. The Timing of Developmental Transitions in Plants. *Cell* **2006**, *125*, 655–664. [CrossRef] [PubMed]
14. Srikanth, A.; Schmid, M. Regulation of flowering time: All roads lead to Rome. *Cell. Mol. Life Sci.* **2011**, *68*, 2013–2037. [CrossRef] [PubMed]

15. Mutasa-Gottgens, E.; Hedden, P. Gibberellin as a factor in floral regulatory networks. *J. Exp. Bot.* **2009**, *60*, 1979–1989. [CrossRef]
16. Huijser, P.; Schmid, M. The control of developmental phase transitions in plants. *Development* **2011**, *138*, 4117–4129. [CrossRef]
17. Okamuro, J.K.; Boer, B.G.W.D.; Lotys-Prass, C.; Szeto, W.; Jofuku, K.D. Flowers into shoots: Photo and hormonal control of a meristem identity switch in *Arabidopsis*. *Proc. Natl. Acad. Sci. USA* **1996**, *93*, 13831–13836. [CrossRef]
18. Gocal, G.F.W.; Sheldon, C.C.; Gubler, F.; Moritz, T.; Bagnall, D.J.; MacMillan, C.P.; Li, S.F.; Parish, R.W.; Dennis, E.S.; Weigel, D.; et al. GAMYB-like Genes, Flowering, and Gibberellin Signaling in *Arabidopsis*. *Plant Physiol.* **2001**, *127*, 1682–1693. [CrossRef]
19. Wilson, R.N.; Heckman, J.W.; Somerville, C.R. Gibberellin Is Required for Flowering in *Arabidopsis thaliana* under Short Days. *Plant Physiol.* **1992**, *100*, 403–408. [CrossRef]
20. Moon, J.; Suh, S.-S.; Lee, H.; Choi, K.-R.; Hong, C.B.; Paek, N.-C.; Kim, S.-G.; Lee, I. TheSOC1MADS-box gene integrates vernalization and gibberellin signals for flowering in *Arabidopsis*. *Plant J.* **2003**, *35*, 613–623. [CrossRef]
21. Eriksson, S.; Böhlenius, H.; Moritz, T.; Nilsson, O. GA4 Is the Active Gibberellin in the Regulation of *LEAFY* Transcription and *Arabidopsis* Floral Initiation. *Plant Cell* **2006**, *18*, 2172–2181. [CrossRef] [PubMed]
22. Blazquez, M.; Green, R.; Nilsson, O.; Sussman, M.; Weigel, D. Gibberellins promote flowering of *Arabidopsis* by activating the *LEAFY* promoter. *Plant Cell* **1998**, *10*, 791–800. [CrossRef] [PubMed]
23. Yamaguchi, N.; Winter, C.M.; Wu, M.-F.; Kanno, Y.; Seo, M.; Wagner, D.; Yamaguchi, A. Gibberellin Acts Positively Then Negatively to Control Onset of Flower Formation in *Arabidopsis*. *Science* **2014**, *344*, 638–641. [CrossRef] [PubMed]
24. Fernández, H.; Fraga, M.; Bernard, P.; Revilla-Bahillo, M.A.M. Quantification of GA1, GA3, GA4, GA7, GA9, and GA20 in vegetative and male cone buds from juvenile and mature trees of *Pinus radiata*. *Plant Growth Regul.* **2003**, *40*, 185–188. [CrossRef]
25. Niu, S.; Yuan, L.; Zhang, Y.; Chen, X.; Li, W. Isolation and expression profiles of gibberellin metabolism genes in developing male and female cones of *Pinus tabuliformis*. *Funct. Integr. Genom.* **2014**, *14*, 697–705. [CrossRef]
26. Duan, D.; Jia, Y.; Yang, J.; Li, Z.-H. Comparative Transcriptome Analysis of Male and Female Conelets and Development of Microsatellite Markers in *Pinus bungeana*, an Endemic Conifer in China. *Genes* **2017**, *8*, 393. [CrossRef]
27. Kong, L.; Von Aderkas, P.; Zaharia, L.I. Effects of Exogenously Applied Gibberellins and Thidiazuron on Phytohormone Profiles of Long-Shoot Buds and Cone Gender Determination in Lodgepole Pine. *J. Plant Growth Regul.* **2015**, *35*, 172–182. [CrossRef]
28. Crain, B.A.; Cregg, B.M. Regulation and Management of Cone Induction in Temperate Conifers. *For. Sci.* **2017**, *64*, 82–101. [CrossRef]
29. Williams, C.G. *Conifer Reproductive Biology*; Springer: Berlin, Germany, 2009; p. 169.
30. Hashizume, H. The effect of gibberellin upon flower formation in *Cryptomeria japonica*. *J. Jpn. For. Soc.* **1959**, *41*, 375–381, (In Japanese with English summary).
31. Hashizume, H. Studies on flower bud formation, flower sex differentiation and their control in conifers. *Bull. Tottori Univ. For.* **1973**, *7*, 1–139, (In Japanese with English summary).
32. Mishima, K.; Hirao, T.; Tsubomura, M.; Tamura, M.; Kurita, M.; Nose, M.; Hanaoka, S.; Takahashi, M.; Watanabe, A. Identification of novel putative causative genes and genetic marker for male sterility in Japanese cedar (*Cryptomeria japonica* D.Don). *BMC Genom.* **2018**, *19*, 277. [CrossRef] [PubMed]
33. Mishima, K.; Fujiwara, T.; Iki, T.; Kuroda, K.; Yamashita, K.; Tamura, M.; Fujisawa, Y.; Watanabe, A. Transcriptome sequencing and profiling of expressed genes in cambial zone and differentiating xylem of Japanese cedar (*Cryptomeria japonica*). *BMC Genom.* **2014**, *15*, 219. [CrossRef] [PubMed]
34. Nose, M.; Watanabe, A. Clock genes and diurnal transcriptome dynamics in summer and winter in the gymnosperm Japanese cedar (*Cryptomeria japonica* (L.f.) D.Don). *BMC Plant Boil.* **2014**, *14*, 308. [CrossRef]
35. Fukuda, Y.; Hirao, T.; Mishima, K.; Ohira, M.; Hiraoka, Y.; Takahashi, M.; Watanabe, A. Transcriptome dynamics of rooting zone and aboveground parts of cuttings during adventitious root formation in *Cryptomeria japonica* D. Don. *BMC Plant Boil.* **2018**, *18*, 201. [CrossRef] [PubMed]

36. Fukui, K.; Wakamatsu, T.; Agari, Y.; Masui, R.; Kuramitsu, S. Inactivation of the DNA Repair Genes *mut*S, *mut*L or the Anti-Recombination Gene *mut*S2 Leads to Activation of Vitamin B1 Biosynthesis Genes. *PLoS ONE* **2011**, *6*, e19053. [CrossRef]
37. Huang, D.W.; Sherman, B.T.; Tan, Q.; Kir, J.; Liu, D.; Bryant, D.; Guo, Y.; Stephens, R.; Baseler, M.W.; Lane, H.C.; et al. DAVID Bioinformatics Resources: Expanded annotation database and novel algorithms to better extract biology from large gene lists. *Nucleic Acids Res.* **2007**, *35*, W169–W175. [CrossRef]
38. Huang, D.W.; Sherman, B.; Tan, Q.; Collins, J.R.; Alvord, W.G.; Roayaei, J.; Stephens, R.M.; Baseler, M.; Lane, H.C.; Lempicki, R. The DAVID Gene Functional Classification Tool: A Novel Biological Module-Centric Algorithm to Functionally Analyze Large Gene Lists. *Genome Boil.* **2007**, *8*, R183. [CrossRef]
39. Untergasser, A.; Cutcutache, I.; Koressaar, T.; Ye, J.; Faircloth, B.C.; Remm, M.; Rozen, S.G. Primer3—new capabilities and interfaces. *Nucleic Acids Res.* **2012**, *40*, e115. [CrossRef]
40. Pfaffl, M.W. A new mathematical model for relative quantification in real-time RT-PCR. *Nucleic Acids Res.* **2001**, *29*, 45. [CrossRef]
41. Gomi, K.; Sasaki, A.; Itoh, H.; Ashikari, M.; Kitano, H.; Matsuoka, M.; Ueguchi-Tanaka, M. GID2, an F-box subunit of the SCF E3 complex, specifically interacts with phosphorylated SLR1 protein and regulates the gibberellin-dependent degradation of SLR1 in rice. *Plant J.* **2004**, *37*, 626–634. [CrossRef]
42. Krizek, B.A.; Fletcher, J.C. Molecular mechanisms of flower development: An armchair guide. *Nat. Rev. Genet.* **2005**, *6*, 688–698. [CrossRef] [PubMed]
43. Becker, A.; Theißen, G. The major clades of MADS-box genes and their role in the development and evolution of flowering plants. *Mol. Phylogenet. Evol.* **2003**, *29*, 464–489. [CrossRef]
44. Ueguchi-Tanaka, M.; Ashikari, M.; Nakajima, M.; Itoh, H.; Katoh, E.; Kobayashi, M.; Chow, T.-Y.; Hsing, Y.-I.C.; Kitano, H.; Yamaguchi, I.; et al. GIBBERELLIN INSENSITIVE DWARF1 encodes a soluble receptor for gibberellin. *Nature* **2005**, *437*, 693–698. [CrossRef]
45. Nakajima, M.; Shimada, A.; Takashi, Y.; Kim, Y.-C.; Park, S.-H.; Ueguchi-Tanaka, M.; Suzuki, H.; Katoh, E.; Iuchi, S.; Kobayashi, M.; et al. Identification and characterization of *Arabidopsis* gibberellin receptors. *Plant J.* **2006**, *46*, 880–889. [CrossRef] [PubMed]
46. Ueguchi-Tanaka, M.; Nakajima, M.; Katoh, E.; Ohmiya, H.; Asano, K.; Saji, S.; Hongyu, X.; Ashikari, M.; Kitano, H.; Yamaguchi, I.; et al. Molecular Interactions of a Soluble Gibberellin Receptor, GID1, with a Rice DELLA Protein, SLR1, and Gibberellin. *Plant Cell* **2007**, *19*, 2140–2155. [CrossRef] [PubMed]
47. Fukazawa, J.; Teramura, H.; Murakoshi, S.; Nasuno, K.; Nishida, N.; Ito, T.; Yoshida, M.; Kamiya, Y.; Yamaguchi, S.; Takahashi, Y. DELLAs function as coactivators of GAI-ASSOCIATED FACTOR1 in regulation of gibberellin homeostasis and signaling in *Arabidopsis*. *Plant Cell* **2014**, *26*, 2920–2938. [CrossRef]
48. Cao, N.; Cheng, H.; Wu, W.; Soo, H.M.; Peng, J. Gibberellin Mobilizes Distinct DELLA-Dependent Transcriptomes to Regulate Seed Germination and Floral Development in *Arabidopsis*. *Plant Physiol.* **2006**, *142*, 509–525. [CrossRef]
49. Hou, X.; Hu, W.-W.; Shen, L.; Lee, L.Y.C.; Tao, Z.; Han, J.-H.; Yu, H. Global Identification of DELLA Target Genes during *Arabidopsis* Flower Development. *Plant Physiol.* **2008**, *147*, 1126–1142. [CrossRef]
50. Zentella, R.; Zhang, Z.-L.; Park, M.; Thomas, S.G.; Endo, A.; Murase, K.; Fleet, C.M.; Jikumaru, Y.; Nambara, E.; Kamiya, Y.; et al. Global Analysis of DELLA Direct Targets in Early Gibberellin Signaling in *Arabidopsis*. *Plant Cell* **2007**, *19*, 3037–3057. [CrossRef]
51. Sun, T.-P. Gibberellin-GID1-DELLA: A Pivotal Regulatory Module for Plant Growth and Development. *Plant Physiol.* **2010**, *154*, 567–570. [CrossRef]
52. Jung, C.J.; Hur, Y.Y.; Yu, H.-J.; Noh, J.-H.; Park, K.-S.; Lee, H.J. Gibberellin Application at Pre-Bloom in Grapevines Down-Regulates the Expressions of *VvIAA9* and *VvARF7*, Negative Regulators of Fruit Set Initiation, during Parthenocarpic Fruit Development. *PLoS ONE* **2014**, *9*, e95634. [CrossRef] [PubMed]
53. Hui, W.-K.; Wang, Y.; Chen, X.-Y.; Zayed, M.; Wu, G. Analysis of Transcriptional Responses of the Inflorescence Meristems in *Jatropha curcas* Following Gibberellin Treatment. *Int. J. Mol. Sci.* **2018**, *19*, 432. [CrossRef] [PubMed]
54. Hartmann, U.; Hohmann, S.; Nettesheim, K.; Wisman, E.; Saedler, H.; Huijser, P. Molecular cloning of *SVP*: A negative regulator of the floral transition in *Arabidopsis*. *Plant J.* **2000**, *21*, 351–360. [CrossRef] [PubMed]
55. Wellmer, F.; Alves-Ferreira, M.; Dubois, A.; Riechmann, J.L.; Meyerowitz, E.M. Genome-Wide Analysis of Gene Expression during Early *Arabidopsis* Flower Development. *PLoS Genet.* **2006**, *2*, e117. [CrossRef]

56. Ferrándiz, C.; Gu, Q.; Martienssen, R.; Yanofsky, M.F. Redundant regulation of meristem identity and plant architecture by *FRUITFULL*, *APETALA1* and *CAULIFLOWER*. *Development* **2000**, *127*, 725–734.
57. Tsubomura, M.; Kurita, M.; Watanabe, A. Determination of male strobilus developmental stages by cytological and gene expression analyses in Japanese cedar (*Cryptomeria japonica*). *Tree Physiol.* **2016**, *36*, 653–666. [CrossRef]
58. Hartweck, L.M. Gibberellin signaling. *Planta* **2008**, *229*, 1–13. [CrossRef]
59. Weiss, D.; Ori, N. Mechanisms of Cross Talk between Gibberellin and Other Hormones. *Plant Physiol.* **2007**, *144*, 1240–1246. [CrossRef]
60. Sun, T.P. The molecular mechanism and evolution of the review GA–GID1–DELLA signaling module in plants. *Curr. Biol.* **2011**, *21*, R338–R345. [CrossRef]
61. Yamaguchi, N.; Wu, M.-F.; Winter, C.M.; Berns, M.C.; Nole-Wilson, S.; Yamaguchi, A.; Coupland, G.; Krizek, B.A.; Wagner, D. A Molecular Framework for Auxin-Mediated Initiation of Flower Primordia. *Dev. Cell* **2013**, *24*, 271–282. [CrossRef]
62. Yamaguchi, N.; Jeong, C.W.; Nole-Wilson, S.; Krizek, B.A.; Wagner, D. AINTEGUMENTA and AINTEGUMENTA-LIKE6/PLETHORA3 Induce *LEAFY* Expression in Response to Auxin to Promote the Onset of Flower Formation in *Arabidopsis*. *Plant Physiol.* **2016**, *170*, 283–293. [CrossRef]
63. Fukaki, H.; Taniguchi, N.; Tasaka, M. PICKLE is required for SOLITARY-ROOT/IAA14-mediated repression of ARF7 and ARF19 activity during *Arabidopsis* lateral root initiation. *Plant J.* **2006**, *48*, 380–389. [CrossRef] [PubMed]
64. Hashizume, H. Chemical regulation of flower-bud formation in conifers. *J. Jpn. For. Soc.* **1968**, *50*, 14–16. (In Japanese)
65. Kohorn, B.D.; Johansen, S.; Shishido, A.; Todorova, T.; Martinez, R.; Defeo, E.; Obregon, P. Pectin activation of MAP kinase and gene expression is WAK2 dependent. *Plant J.* **2009**, *60*, 974–982. [CrossRef] [PubMed]
66. Gan, S.; Amasino, R.M. Making Sense of Senescence. *Plant Physiol.* **1997**, *113*, 313–319. [CrossRef]
67. Uauy, C.; Distelfeld, A.; Fahima, T.; Blechl, A.; Dubcovsky, J. A NAC Gene Regulating Senescence Improves Grain Protein, Zinc, and Iron Content in Wheat. *Science* **2006**, *314*, 1298–1301. [CrossRef]
68. Miao, Y.; Laun, T.; Zimmermann, P.; Zentgraf, U. Targets of the WRKY53 transcription factor and its role during leaf senescence in *Arabidopsis*. *Plant Mol. Biol.* **2004**, *55*, 853–867. [CrossRef]
69. Hu, Y.; Jiang, Y.; Han, X.; Wang, H.; Pan, J.; Yu, D. Jasmonate regulates leaf senescence and tolerance to cold stress: Crosstalk with other phytohormones. *J. Exp. Bot.* **2017**, *68*, 1361–1369. [CrossRef]
70. Zhang, H.; Zhou, C. Signal transduction in leaf senescence. *Plant Mol. Boil.* **2012**, *82*, 539–545. [CrossRef]
71. Jibran, R.; Hunter, D.; Dijkwel, P. Hormonal regulation of leaf senescence through integration of developmental and stress signals. *Plant Mol. Boil.* **2013**, *82*, 547–561. [CrossRef]
72. Zhang, K.; Xia, X.; Zhang, Y.; Gan, S.-S. An ABA-regulated and Golgi-localized protein phosphatase controls water loss during leaf senescence in *Arabidopsis*. *Plant J.* **2011**, *69*, 667–678. [CrossRef] [PubMed]